THE JOURNAL OF BIOLOGICAL CHEMISTRY VOL. 290, NO. 2, pp. 827–840, January 9, 2015
© 2015 by The American Society for Biochemistry and Molecular Biology, Inc. Published in the U.S.A.

A Novel MEK-ERK-AMPK Signaling Axis Controls Chemokine Receptor CCR7-dependent Survival in Human Mature Dendritic Cells*

Received for publication, July 14, 2014, and in revised form, October 31, 2014 Published, JBC Papers in Press, November 25, 2014, DOI 10.1074/jbc.M114.596551

Pilar López-Cotarelo[‡1], Cristina Escribano-Díaz[‡2], Ivan Luis González-Bethencourt[‡], Carolina Gómez-Moreira[‡3], María Laura Deguiz[‡], Jesús Torres-Bacete[‡4], Laura Gómez-Cabañas[‡5], Jaime Fernández-Barrera[‡6], Cristina Delgado-Martín[‡7], Mario Mellado[§], José Ramón Regueiro[¶], María Eugenia Miranda-Carús[‖], and José Luis Rodríguez-Fernández[‡8]

From the [‡]CIB/CSIC (Centro de Investigaciones Biológicas, Consejo Superior de Investigaciones Científicas), 28040 Madrid, the [§]CNB/CSIC (Centro Nacional de Biotecnología/Consejo Superior de Investigaciones Cientificas,) 28049 Madrid, the [¶]School of Medicine, Universidad Complutense, 28040 Madrid, and the [‖]Department of Rheumatology, Hospital La Paz, 28046 Madrid, Spain

Background: Chemokine receptor CCR7 promotes survival in mature dendritic cells (mDCs).
Results: Activated AMP-dependent kinase (AMPK) induces apoptosis in mDCs; CCR7 uses the kinases MEK1/2-ERK1/2 to regulate phosphorylation of AMPK on Ser-485 and consequently its inhibition.
Conclusion: CCR7 uses a novel MEK1/2-ERK1/2-AMPK signaling axis to induce survival in mDCs.
Significance: AMPK is a potential target to regulate mDC-mediated immune responses.

Chemokine receptor CCR7 directs mature dendritic cells (mDCs) to secondary lymph nodes where these cells regulate the activation of T cells. CCR7 also promotes survival in mDCs, which is believed to take place largely through Akt-dependent signaling mechanisms. We have analyzed the involvement of the AMP-dependent kinase (AMPK) in the control of CCR7-dependent survival. A pro-apoptotic role for AMPK is suggested by the finding that pharmacological activators induce apoptosis, whereas knocking down of AMPK with siRNA extends mDC survival. Pharmacological activation of AMPK also induces apoptosis of mDCs in the lymph nodes. Stimulation of CCR7 leads to inhibition of AMPK, through phosphorylation of Ser-485, which was mediated by $G_i/G\beta\gamma$, but not by Akt or S6K, two kinases that control the phosphorylation of AMPK on Ser-485 in other settings. Using selective pharmacological inhibitors, we show that CCR7-induced phosphorylation of AMPK on Ser-485 is mediated by MEK and ERK. Coimmunoprecipitation analysis and proximity ligation assays indicate that AMPK associates with ERK, but not with MEK. These results suggest that in addition to Akt-dependent signaling mechanisms, CCR7 can also promote survival of mDCs through a novel MEK1/2-ERK1/2-AMPK signaling axis. The data also suggest that AMPK may be a potential target to modulate mDC lifespan and the immune response.

Mature dendritic cells (mDCs)[9] are potent antigen-presenting cells that stimulate naive T cells in the lymph nodes (1). It has been shown that the longevity of mDCs importantly affects the immune response. In this regard, both mice depleted of mDCs and mice that present aberrant long lived mDCs develop autoimmune diseases (2–6). However, between these two extremes, it is observed that the immune response improves as the longevity of the mDCs increases (3, 7). The aforementioned results suggest that obtaining information on the mechanisms that regulate mDC survival can be very useful to develop strategies to modulate the longevity of these cells and improve the immune response.

Chemokine receptor CCR7 (ligands CCL19 and CCL21) directs mDCs to the lymph nodes (LNs), attracted first by CCL21, which is expressed in the lymphatic vessels that lead to the LNs, and then by both CCL19 and CCL21, which are both expressed by stromal cells in the LNs (8, 9). Apart from directing the migration of mDCs, CCR7 also promotes survival in

* This work was supported by grants awarded by the Ministerio de Educación y Ciencia (SAF2005-00801), Ministerio de Ciencia e Innovación (SAF2008-01468), Ministerio de Economía y Competitividad (SAF2011-23890), Ministerio de Economía y Competitividad (SAF2011-23890), RIER (RETICS Program/Instituto de Salud Carlos III) (RD08/0075), and Consejería de Educación y Empleo from Comunidad de Madrid (Raphyme, S2010/BMD-2350).
[1] Supported by an FPI scholarship (Ministerio de Economía y competitividad).
[2] Recipient of an I3P contract (Consejo Superior de Investigaciones Científicas-Fondo Social Europeo).
[3] Supported by a contract associated with Grant Raphyme S2010/BMD-2350 (Consejería de Educación y Empleo, Comunidad de Madrid).
[4] Recipient of a JAEdoc contract (Consejo Superior de Investigaciones Científicas-Fondo Social Europeo).
[5] Supported by an FPU scholarship (Ministerio de Educación y Ciencia).
[6] Supported by scholarship I3P intro (Ministerio de Educación y Ciencia).
[7] Partially supported by an FPI fellowship, conferred by the Ministerio de Educación y Ciencia (Spain), and by a contract associated with grant RD08/0075 (RIER).
[8] To whom correspondence should be addressed: Centro de Investigaciones Biológicas, Consejo Superior de Investigaciones Científicas. C/Ramiro de Maeztu, 9, 28040 Madrid, Spain. Tel.: 34-91-8373112, Ext. 4302; Fax: 34-34-91-5360436; E-mail: rodrifer@cib.csic.es.

[9] The abbreviations used are: mDC, mature dendritic cell; ACC, acetyl coenzyme A carboxylase; mTOR, mammalian target of rapamycin; mTORC, mTOR complex; PTX, pertussis toxin; LN, lymph node; PLN, popliteal LN; FOXO, Forkhead box class O; AMPK, AMP-dependent kinase; S6K, S6 kinase; AICAR, 5-aminoimidazole-4-carboxamide ribonucleotide; CFSE, carboxyfluorescein diacetate succinimidyl ester; PLA, proximity ligation assay; DMSO, dimethyl sulfoxide; SR, sulforhodamine B; Z, benzyloxycarbonyl; VAD-FMK, Val-Ala-Asp(OMe)-fluoromethyl ketone; OMe, O-methyl ester; Akti, Akt1/2 inhibitor; RAPA, rapamycin; Abs, antibodies; p, phospho.

these cells (10–12), although the signaling mechanisms that regulate the latter function are starting to be defined. Previously, we showed that CCR7-regulated survival in mDCs is mediated by the G_i family of G proteins and the kinase Akt (10, 11). This kinase promotes survival through activation of the transcription factor NFκB and inhibition of several pro-apoptotic targets, including the transcription factors FOXO1/3 and the kinase GSK3β (10–12).

AMP-dependent kinase (AMPK) is considered a molecular sensor of cellular energy status (13, 14). Under conditions of low cellular energy status, AMPK becomes activated, resulting in the stimulation of ATP-producing (catabolic) pathways and the inhibition of ATP-consuming (anabolic) processes (13, 14), which together lead to the recovery of the ATP/ADP ratio of the cell. Recently, it has emerged that AMPK may also promote survival (*e.g.* Ref. 15) or apoptosis (*e.g.* Ref. 16) depending on the cell type. AMPK is activated upon phosphorylation of Thr-172, which is located on the activation loop of the catalytic α-subunit of the kinase (17), and it is inhibited by phosphorylation of Ser-485/491 (AMPKα1 on Ser-485 and AMPKα2 on Ser-491) (18–20). Phosphorylation of Ser-485/491 blocks the activity of AMPK, even when Thr-172 is phosphorylated, suggesting that phosphorylation of the aforementioned Ser residues exerts a dominant inhibitory role on activity of AMPK (21). It has been shown that the kinases Akt (18, 22, 23) or S6K (21) can inhibit AMPK by directly phosphorylating Ser-485/491 in different cell types. Herein we have studied whether the kinase AMPK plays a role in the regulation of the survival of mDCs. We show, first, that AMPK can play pro-apoptotic roles in mDCs both *in vitro* and *in vivo*; second, we show that the stimulation of CCR7 in mDCs leads to a rapid inhibition of AMPK through the phosphorylation of Ser-485; third, we show that MEK/ERK mediate the CCR7-dependent inhibition of AMPK; and fourth, we show that ERK, but not MEK, interacts with AMPK. Together, these results indicate that CCR7 can contribute to extend the survival of mDCs through the novel MEK1/2-ERK1/2-AMPK signaling axis. These results also suggest that the kinase AMPK may be a potential target to modulate the immune response.

EXPERIMENTAL PROCEDURES

Reagents and Materials—CCL19, CCL21 and TNFα were from PeproTech (Rocky Hill, NJ). GM-CSF and IL4 were purchased from ImmunoTools. Fluorescent dye carboxyfluorescein diacetate succinimidyl ester (CFSE) was obtained from Molecular Probes. FLIVO™ is Val-Ala-Asp(OMe)-fluoromethyl ketone (VAD-FMK). Sulforhodamine B (SR)-FLIVO (SR, λ_{abs} 565 nm; λ_{em} >600 nm), a form of FLIVO conjugated to sulforhodamine B, was obtained from Immunochemistry Technologies, LLC. Z-VAD-FMK was obtained from Enzo (Life Sciences). LY294002, Akt1/2 inhibitor, pertussis toxin, Hoechst 33342, propidium iodide, and the anti-α-tubulin antibodies were from Sigma. Compound C (24), UO126 and PD0325901, and ERK activation inhibitor peptide II, were from Calbiochem (Nottingham, UK). Rapamycin, KU0063794, Gallein, A769662 and FR180204 were obtained from Tocris Bioscience (Bristol, UK). CAY10561 was from Cayman Chemicals (Ann Harbor, MI). The anti-Bim antibody was from Affinity Bioreagents (Golden, CO). The MEK1, β-actin, 4E-BP1, ERK1, ERK2, and anti-AMPKα1 antibodies were from Santa Cruz Biotechnology Inc. (Santa Cruz, CA). The anti-Akt1, anti Bcl-$_{xL}$, anti-AMPKα, the anti-TSC2, anti-mTOR, anti-phospho-MEK1/2 (Ser-217/221), anti-phospho-ERK1/2 (Thr-202/Tyr-204 in ERK1, Thr-185/Tyr-187 in ERK2), anti-phospho-Akt1 (Ser-473), anti-phospho-AMPKα1 (Ser-485), anti-phospho-AMPKα (Thr-172), anti-phospho-TSC2 (Thr-1462), anti-phospho-mTOR (Ser-2448) and anti-phospho-4EBP1 (Thr-37/46), anti-phospho-p70-S6K (Thr-389), and anti-p70-S6K antibodies were from Cell Signaling Technology (Beverly, MA). The anti-phospho-acetyl CoA-carboxylase (Ser-79) was from Millipore. The anti-cleave caspase 3 was form Biorbyt (Cambridge, UK).

Mice—C57BL/6 mice (8–10 weeks) were maintained in the animal facility at the Centro de Investigaciones Biológicas and treated according to Animal Care Committee guidelines.

Purification of Murine DCs and Labeling of the Cells with Fluorescent Cell Trackers—Murine DCs were purified (97% $CD11c^+$) from spleens of donor mice using magnetic beads (Miltenyi) following the manufacturer's protocol. DCs used in the *in vivo* studies were labeled for 30 min at 37 °C with 2.5 μM of the fluorescent cell tracker probe CFSE in 0.1% BSA in PBS.

Cells and Culture Conditions—Human peripheral blood mononuclear cells were isolated from buffy coats from normal donors over a Lymphoprep (Nycomed, Norway). Monocytes were purified using anti-CD14 magnetic beads (Miltenyi) following the manufacturer's protocol and then induced to differentiate to DCs by adding GM-CSF and IL4 for 7 days as indicated previously (10, 11, 25–27). The DCs were induced to mature by adding TNFα as indicated previously (10, 11, 25–27).

Assays of Apoptotic Damage in Vitro—An equal number of live mDCs (determined by exclusion on trypan blue staining) were incubated in 0.1% BSA or 10% FCS in RPMI in the presence or absence of AMPK activators. Subsequently, the mDCs were harvested and plated for 40 min on polyornithine-coated coverslips. Apoptotic nuclear morphology was assessed using Hoechst 33342 staining as indicated previously (10, 11, 25, 26) or by analyzing the loss of nuclear DNA content by flow cytometry using propidium iodide as indicated elsewhere (28, 29).

Cell Lysis and Western Blot Analysis—To reduce the basal levels of activity of the molecules analyzed, mDCs (100×10^3 cells) were maintained in 0.1% BSA/RPMI for 30 min before starting the stimulation with chemokines. Mature DCs were then stimulated with chemokines for the indicated periods of time. The stimulation was terminated by solubilizing the cells in SDS-PAGE sample buffer (100 mM Tris/HCl, pH 6.8, 0.05 mM sodium orthovanadate, 3% SDS, 1 mM EDTA, 2% 2-β-mercaptoethanol, 5% glycerol) and boiled and then fractionated by SDS-PAGE and transferred to nitrocellulose membranes. After blocking with 5% nonfat milk protein in TBST (TBS plus 0.1% Tween 20), pH 7.5, membranes were incubated with the indicated antibodies in TBST and visualized with the appropriate HRP-conjugated secondary antibodies (Santa Cruz Biotechnology) and an ECL substrate (Pierce) detection system. Quantification of the blots was performed using MultiGauge software from Fujifilm.

Immunoprecipitation—Mature DC ($\sim 50 \times 10^6$ DCs) were dissolved in lysis buffer A (1% Nonidet P-40, 100 mM NaCl, 1 mM EDTA, 0.5 μM vanadate, and 20 mM Hepes, pH 7.4, includ-

ing a protease inhibition mixture (Sigma), and subjected to immunoprecipitation with anti-AMPKα antibody in the presence of TrueBlot™ anti-rabbit Ig agarose beads (TrueBlot™, eBioscience, San Diego, CA). Immunoprecipitates were washed five times in lysis buffer and then boiled in SDS-PAGE sample buffer supplemented with 50 mM dithiothreitol. After SDS-PAGE and transfer to nitrocellulose, the primary antibody step was followed by incubation with a horseradish peroxidase-conjugated antibody that recognizes native rabbit IgG (TrueBlot™, eBioscience).

SiRNAs and Nucleofections—Random control and AMPKα1 siRNAs were obtained from Santa Cruz Biotechnology. The siRNAs were transfected into mDCs by using nucleofection technology (Amaxa Biosystems) according to the manufacturer's instructions.

Proximity Ligation Assay (PLA)—The assay was performed on mDC seeded onto polyornithine-coated coverslips. The mDCs were treated with CCL21 and fixed in 4% paraformaldehyde. Staining with primary antibodies was performed as in conventional immunofluorescence. However, instead of using fluorescently labeled secondary antibodies, a PLA was carried following the manufacturer's instructions (30) (Duolink II *in situ* PLA detection kit, Olink Bioscience). Briefly, samples were incubated with secondary antibodies conjugated with DNA probes (MINUS and PLUS DNA probes). Probes were hybridized and ligated, followed by amplification of the DNA template in a rolling circle amplification reaction. A detection solution was added to identify amplified DNA. Finally, coverslips with the cells were prepared using mounting medium that includes DAPI to stain the nuclei. The coverslips were analyzed with a confocal microscope, and the interactions among ERK and AMPK proteins, detected as distinct fluorescent spots inside each DC, were subsequently quantified.

Two-photon Microscopy and Analysis of Apoptotic CFSE-labeled Dendritic Cells in the Lymph Nodes—The method has been described in detail previously (10, 25, 26, 31). Briefly, CFSE-labeled splenic mDCs (10^8 mDCs/ml) were dissolved in 20 μl of RPMI and injected subcutaneously along with LPS (1 μg/ml) into the hind footpad of recipient C57BL/6 mice (2×10^6 mDCs per footpad). After 36 h, when the mDCs have already reached the popliteal LNs (PLNs) (26, 32), treated or control animals were injected intraperitoneally, respectively, with the AMPK activator A769662 (3.6 mg/25 g of mice in DMSO) or with vehicle control DMSO. 40.5 h after initiation of the experiment, the mice were injected intravenously with SR-FLIVO (SR, λ_{abs} 565 nm; λ_{em} >600 nm), and after an additional 1 h, the mice were sacrificed, and the popliteal LNs were extracted from the mice and subsequently subjected to two-photon confocal analysis to visualize among the injected CFSE-mDCs those that present SR-FLIVO staining (see "Results"). Two-photon microscopy and analysis of apoptotic CFSE-DCs in the LNs was performed as described previously (31).

Statistics—Data are expressed as mean ± S.D., and significance of differences between two series of results was assessed using the Student's *t* test. Values of $p < 0.05$ were considered significant, and *ns* indicates non-significant differences.

RESULTS

AMPK Promotes Apoptosis in Mature Dendritic Cells in Vitro—To determine whether AMPK could regulate apoptosis in mDCs, we maintained the cells in complete medium in the absence or in the presence of the selective AMPK activators A769662 or AICAR. A769662 is a direct allosteric activator of AMPK (36). AICAR is an agent that is transported into cells where it is phosphorylated to form the AMP-mimetic *S*-aminoimidazole-4-carboxamida ribonucleoside monophosphate (ZMP), which activates AMPK without altering the intracellular levels of AMP or ATP (33) (Fig. 1*A*). Western blotting analysis using antibodies that recognize a phosphorylated/active AMPKα (p-AMPK (Thr-172)), or phosphorylated acetyl coenzyme A carboxylase (ACC) (p-ACC (Ser 79)), which is a direct target of active AMPK (34), confirmed that the treatment of mDCs with A769662 or AICAR induced activation of AMPK (Fig. 1*A*, *panel a*). We treated the mDCs with the AMPK activators and then measured the percentage of apoptosis by staining the nuclei of the cells with Hoechst 33342. DCs treated with Akti1/2, a potent inhibitor of the pro-survival kinase Akt (10, 11, 25), were used as positive controls of apoptosis. As shown in Fig. 1*A*, *panels b* and *c*, mDCs treated with pharmacological activators of AMPK displayed increased percentage of apoptosis. Similar results were obtained when, instead of Hoechst staining, apoptosis was measured by analyzing the loss of nuclear DNA content typical of apoptotic cells by flow cytometry using propidium iodide as label (28, 29) (Fig. 1*A*, *panel d*) or the activation of caspase-3, another well known apoptotic marker (Fig. 1*A*, *panel e*). When the pharmacological activators of AMPK were used to induce apoptosis in mDCs that had been pretreated with Z-VAD-FMK, a general caspase inhibitor, the effects of the AMPK activators on the apoptosis of the cells were abrogated, indicating that these agents induce caspase-dependent cell death (Fig. 1*B*). Finally, to corroborate that AMPK played pro-apoptotic roles in DCs, we reduced AMPK levels using siRNA (Fig. 1*C*, *panel a*). When DCs with normal or reduced levels of AMPK were shifted to 0.1% BSA/RPMI for 24 h and then stained with Hoechst 33342, it was observed that the mDCs that displayed reduced levels of AMPK (Fig. 1*C*, *panel b*) also presented a reduced percentage of apoptosis. Together, these results indicate that AMPK can promote apoptosis in mDCs.

We analyzed potential mechanisms whereby active AMPK could induce apoptosis in DCs. Previously, we reported that the kinase GSK3β may induce apoptosis in DCs by promoting the translocation to the nucleus of the transcription factor FOXO (10), which controls the expression of the pro-apoptotic Bcl2 family member Bim (10, 25, 26, 35). We tested whether similarly active AMPK could also promote the translocation of FOXO and induce overexpression of Bim in DCs. For this purpose, we transfected the DCs with FOXO1-GFP and then induced activation of AMPK by stimulating the DCs with AICAR or A769662. As shown in Fig. 2*A*, these agents induced a significant increase in the number of DCs that displayed FOXO-GFP in the nucleus. Consistent with these results, the stimulation of DCs with AICAR or A769662 also caused an increase in Bim levels in the DCs (Fig. 2*B*). In similar experi-

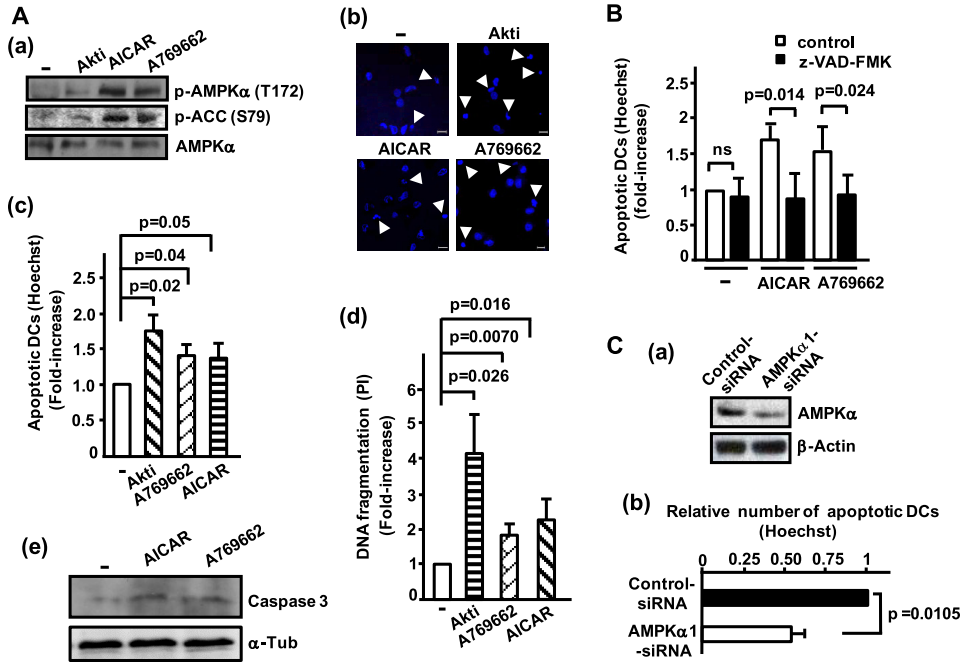

FIGURE 1. **AMPK induces apoptosis in dendritic cells.** *A*, *panel a*, DCs were suspended in 10% FCS in RPMI and then incubated for 24 h either in this medium alone (−) or in this medium plus Akti (5 μM), AICAR (1 mM), or A769662 (25 μM). Aliquots of DCs were subjected to a Western blotting analysis with Abs against phospho-AMPKα (Thr-172), phospho-ACC, or total AMPKα. *Panel b*, photographs taken from representative samples of the Hoechst 33342 stained DCs treated as in *panel a*. *Arrowheads* indicate apoptotic cells, showing condensed or fragmented nuclei. *Panel c*, DCs were suspended in 10% FCS in RPMI and then incubated in medium alone (−) or in medium plus Akti, AICAR, or A769662, as in *panel a*. The number represents -fold increase in the number of apoptotic DCs, determined by Hoechst 33342 staining, with respect to the control untreated DCs kept in 10% FCS in RPMI, which was considered as 1. Results shown represent the mean ± S.D. ($n = 4$). *Panel d*, the cells were treated or not with Akti, AICAR, or A769662 as in *panel b*. The number represents -fold increase in the number of DCs that presented DC fragmentation upon propidium iodide (*PI*) staining with respect to control untreated DCs kept in 10% FCS in RPMI. Results shown represent the mean ± S.D. ($n = 6$). *Panel e*, the DCs were suspended in 10% FCS in RPMI and then incubated for 33 h either in this medium alone (−) or in this medium plus AICAR or A769662 as in *panel a*. Aliquots of DCs were subjected to a Western blotting analysis with an antibody against caspase-3. The blots were probed with an antibody against α-tubulin to show equal loading. A representative experiment out of two performed is shown. *B*, DCs were suspended in 0.1% BSA in RPMI and then incubated for 40 h either in this medium alone (−) or in medium including AICAR (1 mM) or A769662 (25 μM), either in the absence (*control*) or in the presence of 10 μg/ml pan caspase inhibitor z-VAD-FMK. The apoptotic DCs observed in medium alone (−) untreated with z-VAD-FMK were given an arbitrary value of 1, and the -fold increase of apoptosis in the other samples was referred to this value. Results shown represent the mean ± S.D. ($n = 5$). *ns* indicates non-significant differences. *C*, mDCs were nucleofected either with random siRNA (control siRNA) or with a siRNA specific for AMPK (AMPKα1 siRNA). *Panel a*, 36 h after nucleofection, mDCs were washed in RPMI, and then an equal number of live DCs, determined by trypan blue exclusion, were subjected to Western blotting with an anti-AMPKα antibody. To confirm equal loading, the blots were reprobed with an antibody reacting with β-actin. *Panel b*, samples of DCs nucleofected either with control or with AMPKα1 siRNA were washed in RPMI, and then an equal number of live DCs, determined by trypan blue exclusion, were transferred to 0.1% BSA in RPMI for an additional 24 h. At the end of this period, the DCs were stained with Hoechst. The number of apoptotic DCs observed in the control siRNA nucleofected DCs was given an arbitrary value of 1, and the number of apoptotic DCs observed in AMPK siRNA-transfected DCs was referred to this value. Results shown represent the mean ± S.D. ($n = 3$).

ments, we did not observe any change in the expression of the pro-survival Bcl2 member Bcl-$_{xL}$ (not shown). Together, these results suggest that AMPK could induce apoptosis in DCs by promoting translocation of pro-apoptotic FOXO1 to the nucleus, which up-regulates the expression of the pro-apoptotic Bim.

Because it has been shown that AMPK inhibits the kinase mammalian target of rapamycin complex 1 (mTORC1) (36, 37), and mTORC1 has been shown to mediate the pro-survival signaling of the kinase Akt (38), we hypothesized that active AMPK may induce apoptosis by interfering with the pro-survival signaling induced from mTORC1 in DCs. To test this concept first, we analyzed whether mTORC1 plays a pro-survival role in DCs. Inhibition of mTORC1 by treating the DCs with the highly selective inhibitor rapamycin (RAPA) induces apoptosis, indicating that mTORC1 promotes survival in these cells (Fig. 2*C*). Next we studied whether CCR7 could also induce activation of mTORC1. As shown in Fig. 2*D*, simulation of CCR7 with CCL21 induces phosphorylation/inhibition of the mTORC upstream inhibitory molecule TSC2 and an increase in the phosphorylation of 4EBP1, a direct downstream target of mTORC (Fig. 2*D*), together indicating that CCR7 induces activation of mTORC1. Finally, we analyzed whether active AMPK could inhibit CCR7-dependent activation of mTORC1 (Fig. 2*E*). The treatment of the DCs with A769662 or AICAR, which, as indicated by the elevated levels of active/phosphorylated AMPK (Thr-172), induced activation of AMPK (Fig. 2*E*), also inhibited mTORC1 activity, as indicated by the reduction in the phosphorylation of 4EBP1 (Fig. 2*E*). Together, these results indicate that in DCs, active AMPK may also promote apoptosis by inhibiting mTORC1.

Stimulation of CCR7 Receptor Induces Phosphorylation/Inhibition of AMPK—As we have shown previously that stimulation of CCR7 protects mDCs from apoptosis (10, 11), we hypothesized that this receptor could also induce inhibition of pro-apoptotic AMPK in these cells. To test this hypothesis, the mDCs were treated with CCL21 for various times and then lysed in sample buffer. Subsequently, we examined the activity of AMPK using an antibody that recognizes the phosphorylated/inactive form of AMPKα1 (p-Ser-485). Stimulation with

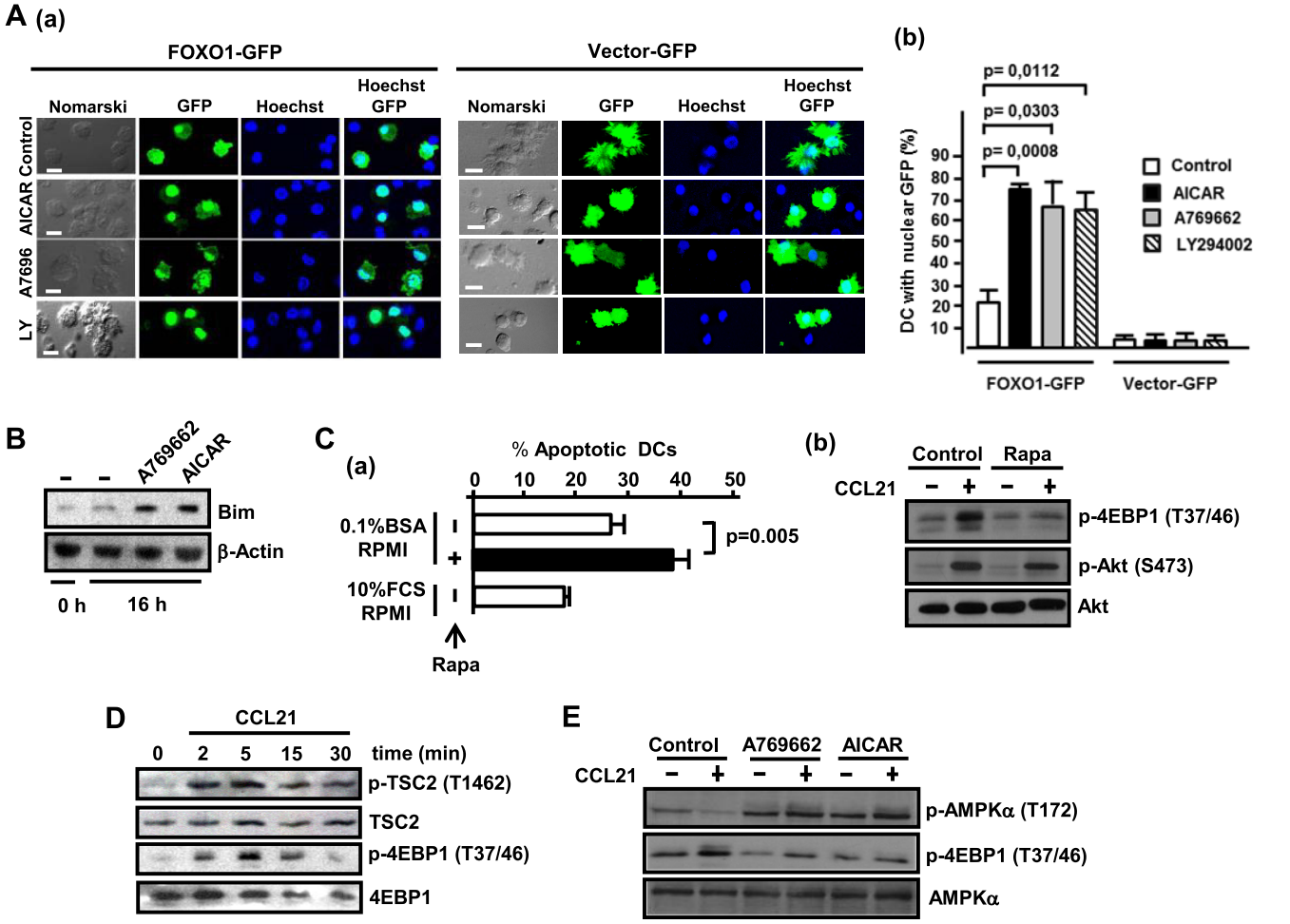

FIGURE 2. **Active AMPK may promote apoptosis by inducing translocation of FOXO1 to the nucleus and by inhibiting mTORC1.** *A*, *panel a*, the DCs were transfected with vector or FOXO1-GFP, and 6 h after transfection, the cells were resuspended in 10% FCS RPMI and then either kept untreated (*Control*) or treated with AICAR (1 mM), A769662 (25 μM), or LY294002 (*LY*, 100 μM) for an additional 2.5 h. Subsequently, the DCs were plated onto polyornithine-coated coverslips, fixed, permeabilized, and stained with Hoechst 33342. The DCs were examined with a fluorescence microscope. *Scale bar* represents 20 μm. *Panel b*, bar diagram representing the percentage of vector- or FOXO1-GFP-transfected DCs with GFP staining concentrated in the nucleus. Results shown represent the mean ± S.D. ($n = 3$). *B*, DCs were suspended in 0.1% BSA in RPMI and then kept untreated (−) or stimulated with A769662 (25 μM) or AICAR (1 mM) for 16 h. Aliquots of the DCs were subjected to a Western blot with an Ab against Bim. Blots were reprobed with an antibody reacting with β-actin to show equal loading (a representative experiment is shown). *C*, *panel a*, the DCs were suspended in 0.1% BSA in RPMI and then treated (+) or not (−) for 40 h with RAPA (100 nM). DCs maintained in 10% FCS in RPMI were used as negative controls. The DCs were plated on polyornithine-coated coverslips, fixed, and stained with Hoechst, and the apoptotic cells were examined as indicated under "Experimental Procedures." Results shown represent the mean ± S.D. ($n = 3$). *Panel b*, to confirm that RAPA inhibited mTORC1, aliquots of the control or RAPA-treated DCs from *panel a* were stimulated (+) or not (−) with CCL21 (15 nM). Subsequently, the DCs were lysed and analyzed by SDS-PAGE, followed by Western blotting. The blots were analyzed with Abs against phosphorylated 4EBP1 (Thr-37/46) or phosphorylated Akt (Ser-473). To show equal loading, the membranes were reprobed with an Ab against Akt. *D*, DCs (100,000 cells), suspended in 0.1% BSA in RPMI, were stimulated for the indicated times with CCL21 (15 nM) and then lysed and analyzed by SDS-PAGE, followed by Western blotting with Abs against phosphorylated TSC2 (Thr-1462) or phosphorylated 4EBP1 (Thr-37/46). To show equal loading, the membranes were reprobed with Abs against total 4EBP1. A representative experiment out of three performed is shown. *E*, the DCs were suspended in 0.1% BSA in RPMI and then kept untreated (*Control*) or treated with A769662 (25 μM) or AICAR (1 mM) for 60 min. Subsequently, the DCs were stimulated (+) or not (−) with CCL21 (15 nM) and then lysed and analyzed by SDS-PAGE, followed by Western blotting. The blots were analyzed with Abs against phosphorylated 4EBP1 (Thr-37/46) or phosphorylated AMPKα (Thr-172). To show equal loading, the membranes were reprobed with an Ab against AMPKα.

CCL21 (Fig. 3*A*) or CCL19 (not shown) induced inactivation of AMPK, which remained at relatively high levels until 60 min and only decayed after 120 min (Fig. 3*A*). Consistent with these results, stimulation of CCR7 caused also a reduction of the phosphorylation of the AMPK substrate ACC (Fig. 3*B*). When we used an antibody that recognizes the active form of AMPK (p-Thr-172), it was observed that stimulation of CCR7 also led to reduced levels of this active form of AMPK (Fig. 3*B*). Finally, the treatments of the mDCs with Compound C, a selective inhibitor of AMPK (24), blunted the phosphorylation of the active form of AMPK (p-Thr-172) (Fig. 3*C*, *panel a*), but failed to affect the CCR7-induced phosphorylation of Ser-485 on AMPK (Fig. 3*C*, *panel b*). Because AMPK activity is completely blunted after the treatment with Compound C, these results indicate that upon stimulation of CCR7, the phosphorylation of AMPK on Ser-485 was not due to an autophosphorylation event, but to the activity of an upstream kinase. In summary, these experiments indicate that stimulation of CCR7 in mDC causes phosphorylation on Ser-485 and inhibition of AMPK, which is mediated by an upstream kinase.

Activation of AMPK Induces Apoptosis of Murine DCs in the Lymph Nodes—We studied whether active AMPK could also play a pro-apoptotic role in the LNs, the setting where DCs present antigens to naive T-cells during the initiation of the

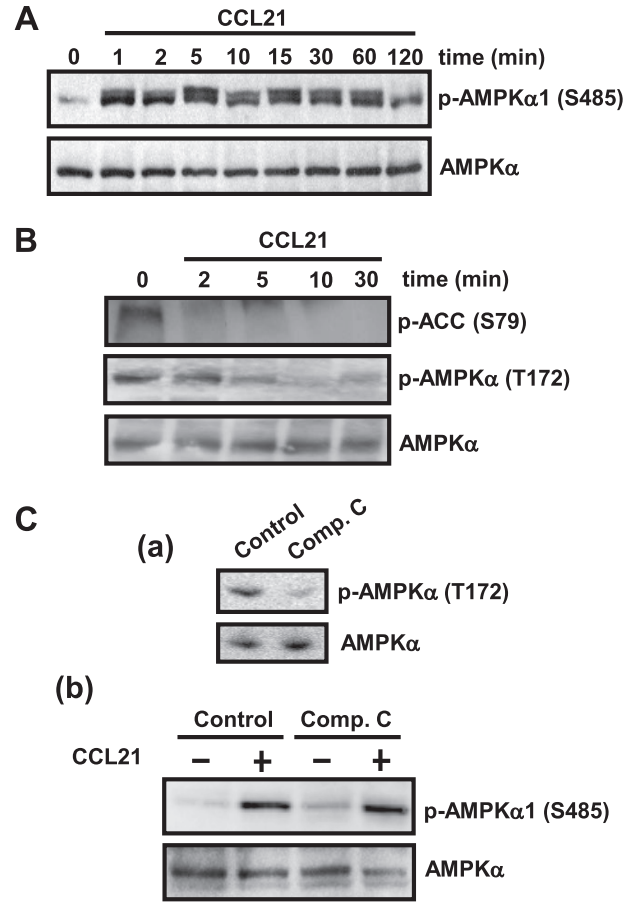

FIGURE 3. **Stimulation of CCR7 induces phosphorylation/inhibition of AMPK.** *A*, DCs (100,000 cells), suspended in 0.1% BSA in RPMI, were stimulated for the indicated times with CCL21 (15 nM) and then lysed and analyzed by SDS-PAGE, followed by Western blotting with Abs against phosphorylated/inhibited AMPKα1 (Ser-485). To show equal loading, the membranes were reprobed with Abs against total AMPKα. A representative experiment out of three performed is shown. *B*, DCs (100,000 cells), suspended as in *A*, were stimulated with CCL21 for the indicated times and then extracted and subjected to a Western blotting with Ab against phospho-ACC (Ser-79) and against phosphorylated/active AMPKα (Thr-172). To show equal loading, the membrane was reprobed with an Ab against total AMPKα. A representative experiment out of three performed is shown. *C*, *panel a*, DCs, suspended as in *panel a*, were either untreated (*Control*) or treated with AMPK inhibitor Compound C (*Comp. C*, 20 μM) for 60 min. Control and Compound C-treated DCs were stimulated with CCL21 (15 nM) for 5 min, and subsequently, lysed and subjected to Western blot analysis with Abs against phospho-AMPKα (Thr-172) and AMPKα. A representative experiment out of three performed is shown. *Panel b*, aliquots of the control or Compound C-treated samples, stimulated or not with CCL21, were used to analyze the activity of AMPK using the anti-phosphorylated AMPKα1 (Ser-485) antibody. To show equal loading, the membrane was reprobed with an Ab against total AMPKα.

immune response. Before performing the experiment *in vivo*, we first analyzed whether the treatment with AMPK activators also induced apoptosis in the splenic mDCs *in vitro*. Treatment with AICAR and A769662 significantly enhanced the activity of AMPK (Fig. 4*A*, *panel a*) and the apoptosis of the cells (Fig. 4*A*, *panel b*), indicating that active AMPK is also pro-apoptotic in splenic mDCs in culture. Furthermore, stimulation of splenic mDCs with murine CCL19 or CCL21 also induced, as in human mDCs, phosphorylation of AMPK on Ser-485 (Fig. 4*B*).

As it is known that conventional mDCs that arrive from peripheral tissues to the LNs become largely apoptotic in these regions (26, 39), we studied whether activators of AMPK could enhance the percentage of apoptotic mDCs inside the PLNs, which would indicate that active AMPK plays pro-apoptotic roles in these cells *in vivo*. For this purpose, C57BL/6 mice were injected subcutaneously in the hind footpad with CFSE-labeled splenic DCs. After 36 h, a time at which, as we previously demonstrated (26), there are a significant number of CFSE-labeled DCs positioned in the PLNs, the mice were injected intraperitoneally with 100 μmol of A769662. Control animals were injected with the same amount of vehicle (Fig. 4*C*, *panel a*). After an additional 4.5 h, the animals were injected intravenously with SR-FLIVO, a poly-caspase binding inhibitor probe (VAD-FMK) conjugated to a fluorescent dye that binds irreversibly to apoptotic caspases and allows the detection of apoptotic cells *in vivo* (10, 25, 26, 31). 1 h after the injection of SR-FLIVO, the mice were sacrificed, and the PLNs were obtained and analyzed by two-photon microscopy. In these experiments, if AMPK is pro-apoptotic, an enhanced SR-FLIVO staining in the mDCs in the PLNs obtained from the A769662-treated animals would be expected when compared with the vehicle-treated controls. Consistent with this prediction, mice injected with A769662 displayed a significant increase in the percentage of SR-FLIVO-labeled CFSE-DCs, indicating that active AMPK plays pro-apoptotic roles in the mDCs *in vivo* (Fig. 4*C*, *panels b* and *c*). We also observed induction of apoptosis in the DCs inside the PLNs when the mice were injected with AICAR (not shown). In summary, the prior experiments indicate that active AMPK promotes apoptosis of mDCs both *in vivo* and *in vitro*.

CCR7-dependent Inhibition of AMPK in mDCs Is Mediated by G_i and Gβγ, but Not by PI3K/Akt or S6K—In the next experiments, we studied the signaling pathway that could regulate the phosphorylation/inhibition of AMPK downstream of CCR7. As the G_i protein family of G proteins and the Gβγ dimers associated to these proteins mediate CCR7-dependent survival in mDCs (10, 11), we tested their involvement in the control of CCR7-dependent inhibition of AMPK. G_i-mediated signaling was blocked by treating the mDCs with the selective inhibitor pertussis toxin (PTX), and Gβγ-mediated signaling was blocked by treating the cells with Gallein (40). The observed inhibition of the CCR7-dependent phosphorylation of ERK1/2 (Fig. 5*A*, *panels a* and *b*), two kinases known to be regulated by G_i and Gβγ (10, 27), indicated that both PTX and Gallein efficiently blocked their targets. The treatment with PTX or Gallein also blunted the CCR7-induced phosphorylation of AMPK on Ser-485 (Fig. 5*A*, *panels a* and *b*), indicating that G_i and Gβγ regulate the phosphorylation of AMPK on Ser-485 downstream of CCR7.

Stimulation of CCR7 induces activation of Akt in mDCs (10, 11, 41), which is also controlled by the G_i family of proteins (10, 11). As Akt mediates the phosphorylation of Ser-485 on AMPK in a variety of cell types (18, 22, 23, 42), we analyzed whether it could also play a similar role downstream of CCR7 in mDCs. Surprisingly, the blocking of the activity of Akt, with the PI3K inhibitor LY294002 (Fig. 5*B*, *panel a*) or with the selective Akt inhibitor Akti1/2 (43) (Fig. 5*B*, *panel b*), failed to affect CCR7-dependent phosphorylation of AMPK on Ser-485, indicating that Akt does not mediate CCR7-dependent inhibition of AMPK in mDCs. Further emphasizing that Akt and AMPK are

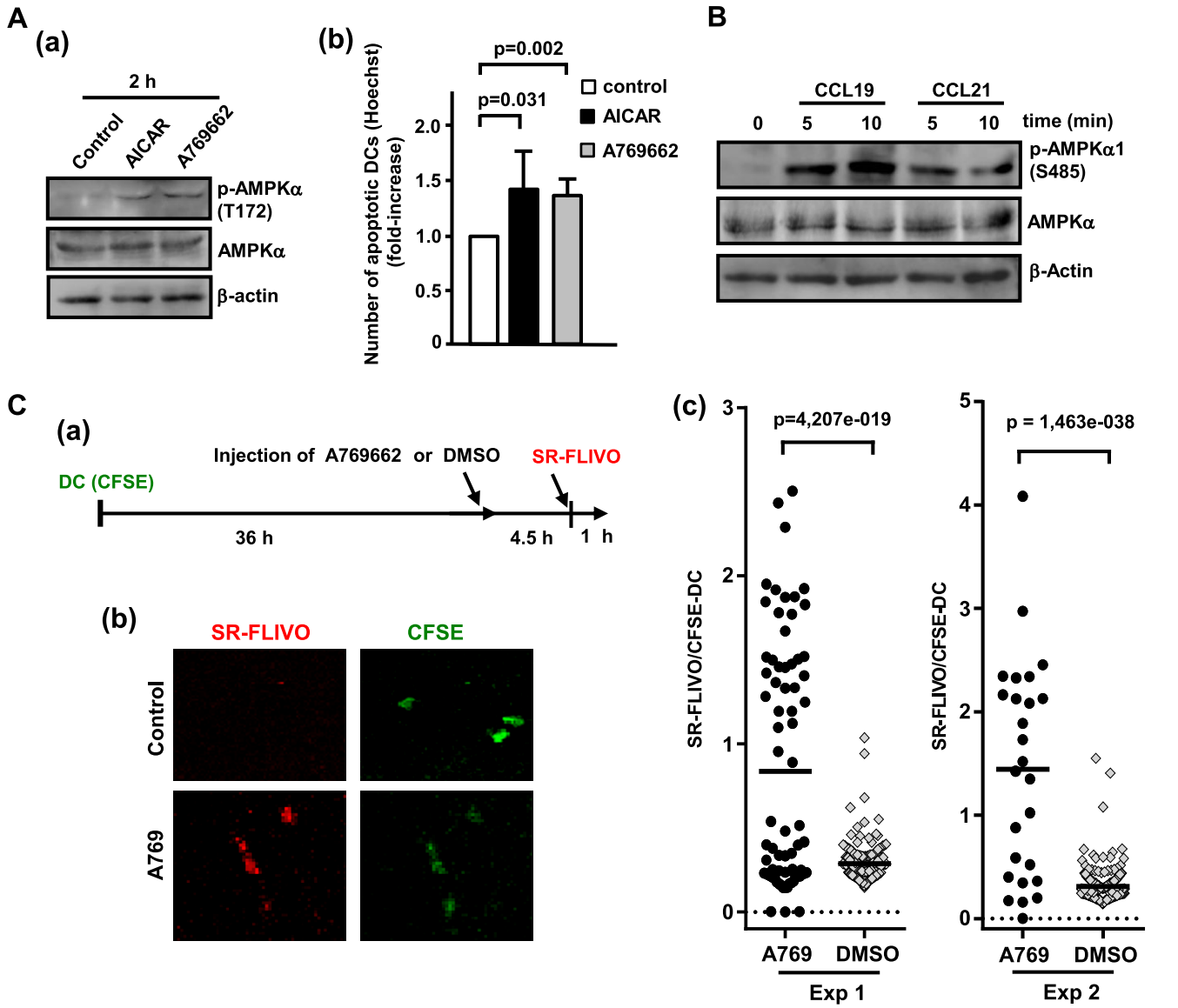

FIGURE 4. **Activation of AMPK increases the apoptosis of dendritic cells *in vitro* and in the lymph nodes.** *A*, *panel a*, splenic mDCs (500,000 cells) suspended in 10% FCS in RPMI were kept unstimulated (*Control*) or stimulated for the indicated times with AICAR (1 mM) or A769662 (25 μM) and then lysed and analyzed by SDS-PAGE, followed by Western blotting with Abs against phospho-AMPKα (Thr-172), total AMPKα and β-actin. A representative experiment out of five performed is shown. *Panel b*, aliquots of the splenic DCs treated as in *panel a* for 2 h were fixed and stained with Hoechst 33342 to detect apoptotic DCs. The number represents the -fold increase in the number of apoptotic DCs respect to the number of apoptotic DCs observed in the controls that was considered as 1. Results represent the mean ± S.D. ($n = 6$ experiments). *B*, splenic DCs (500,000 cells) suspended in 0.1% BSA in RPMI were stimulated for the indicated times with murine CCL19 or CCL21 (both at 15 nM) and then lysed and analyzed by SDS-PAGE, followed by Western blotting with Abs against phospho-AMPKα1 (Ser-485), total AMPKα, and β-actin. A representative experiment out of five performed is shown. *C*, *panel a*, experimental protocol. 2×10^6 CFSE-labeled splenic DCs were injected in the footpads of recipient mice. After 36 h, the animals were injected intraperitoneally with 100 μmol of A769662 or a similar volume of vehicle DMSO. After an additional 4.5 h, mice were injected (intravenously) with SR-FLIVO to stain apoptotic DCs in the LNs. After 1 h, the popliteal LNs were extracted, fixed, and subjected to two-photon analysis. *Panel b*, representative SR-FLIVO staining displayed by CFSE-labeled DCs obtained from the LNs of animals treated either with A769662 or with DMSO. The LNs of the mice were extracted and studied by two-photon microscopy as indicated under "Experimental Procedures." *Panel c*, the stacks of optical images of the LNs were examined with the Leica confocal software, and the values of the maximum amplitude of the SR-FLIVO and CFSE channel were obtained as indicated previously (see "Experimental Procedures"). Data from two experiments are presented. The data are represented as maximum intensity of SR-FLIVO over maximum intensity of CFSE for each individual DC in an LN. For A769662-treated animals, 74 DCs were analyzed in Experiment 1 (*Exp 1*), and 26 DCs were analyzed in Experiment 2 (*Exp 2*); for DMSO vehicle-treated animals, 171 DCs were analyzed in Experiment 1 (*Exp 1*), and 237 DCs were analyzed in Experiment 2(*Exp 2*).

independently regulated, the inhibition of AMPK, by treating the mDCs with Compound C, did not affect the CCR7-dependent phosphorylation of Akt (not shown).

Stimulation of CCR7 also induces activation of the mammalian target of rapamycin complex 1 (mTORC1) (Fig. 5*C*), which promotes survival in mDCs (Fig. 2*C*). Recently, it has been shown that S6K, a molecule that is regulated by mTORC1 (44), may also directly phosphorylate AMPK on Ser-485 (21). Therefore, we studied whether inhibition of S6K could block CCR7-dependent phosphorylation of AMPK on Ser-485. To inhibit S6K, we treated the mDCs with pharmacological agents that block either Akt (Akti) or mTORC1 (RAPA or KU0063794), both upstream regulators of S6K (44) (Fig. 5*D*). To analyze S6K activity, we used an antibody that recognizes a phosphorylated/

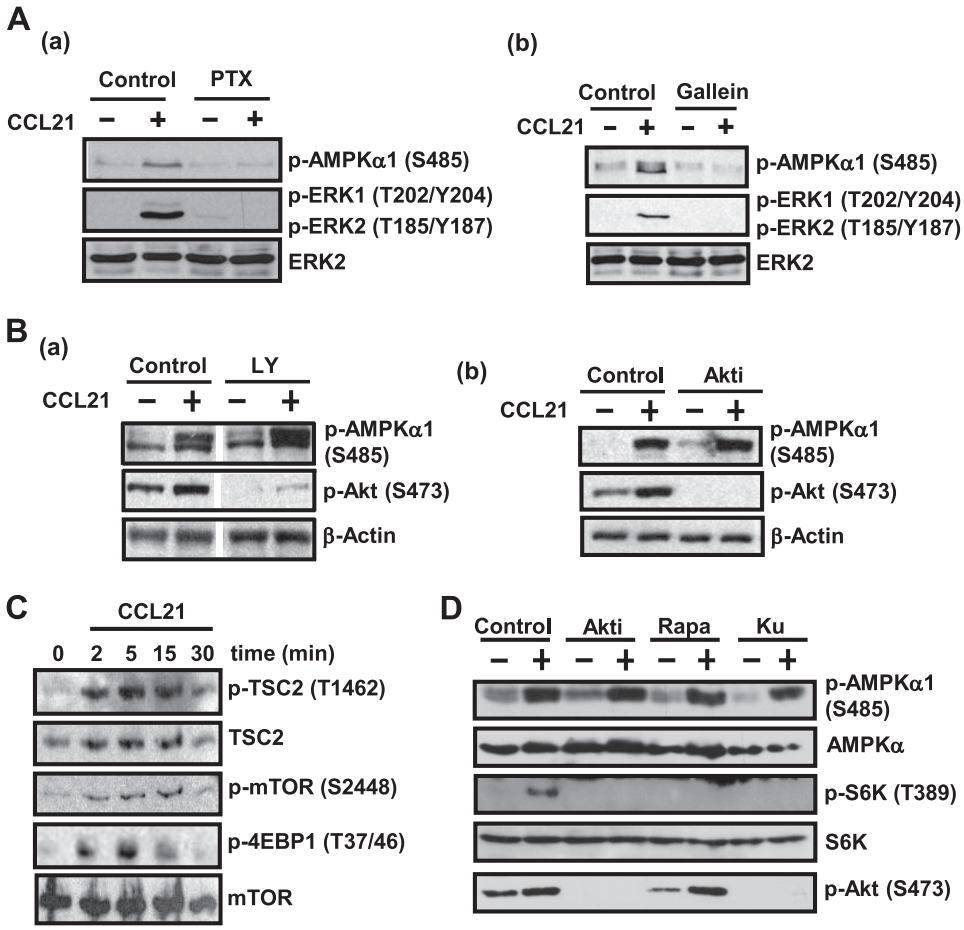

FIGURE 5. **Signaling downstream of CCR7 regulating the phosphorylation of AMPKα1 on serine 485.** *A*, *panel a*, DCs (100,000 cells) in complete medium were either kept untreated (*Control*) or treated with PTX (100 ng/ml) for 180 min. Subsequently, the DCs were washed and suspended in 0.1% BSA in RPMI. Control and PTX-treated DCs were stimulated with CCL21 (15 nM) for 5 min and subsequently lysed and subjected to Western blotting with the Ab against phosphorylated AMPKα1 (Ser-485) or phosphorylated ERK1/2 (Thr-202/Tyr-204 ERK1/Thr-185/Tyr-187 ERK2). ERK2 levels show equal loading of the gels. A representative experiment out of three performed is shown. *Panel b*, DCs, untreated or pretreated with the Gβγ inhibitor Gallein (40) for 15 min, were stimulated or not with CCL21 for 5 min and then lysed, and aliquots were subjected to Western blotting with an Ab against phosphorylated AMPKα1 (Ser-485) and phosphorylated ERK1/2 as in *panel a*. ERK2 levels show equal loading of the gels. A representative experiment out of three performed is shown. *B*, DCs suspended in 0.1% BSA in RPMI were either left untreated (*Control*) or pretreated for 60 min with the PI3K inhibitor LY294002 (*LY*, 100 μM, 60 min) (*panel a*) or Akti (5 μM) (*panel b*). The DCs were subsequently stimulated or not with CCL21 (15 nM) for 5 min and then lysed, and aliquots were subjected to Western blot with the Ab against phosphorylated/inhibited AMPKα1 (Ser-485) or against phosphorylated/active Akt1 (Ser-473). β-Actin levels show equal loading of the gels. A representative experiment out of three performed is shown. *C*, DCs (100,000 cells), suspended in 0.1% BSA in RPMI, were stimulated for the indicated times with CCL21 (15 nM) and then lysed and analyzed by SDS-PAGE, followed by Western blotting with Abs against phosphorylated TSC2 (Thr-1462), phosphorylated mTOR (Ser-2448), or phosphorylated 4EBP1 (Thr-37/46). To show equal loading, the membranes were reprobed with Abs against total TSC2 and mTOR. *D*, DCs suspended in 0.1% BSA in RPMI were either left untreated (*Control*) or pretreated for 60 min with Akti (5 μM), RAPA (100 nM), or KU0063794 (*Ku*) (500 nM). The DCs were subsequently stimulated or not with CCL21 (15 nM) for 5 min. The DCs were then lysed and analyzed by Western blotting with Abs against phosphorylated/inactive AMPKα1 (Ser-485), phosphorylated/active S6K (Thr-389), and phosphorylated/active Akt (Ser-473). Membranes were also probed with antibodies that recognize total S6K and AMPKα.

active form of this kinase (p-S6K (Thr-389)). Treatment of the mDCs with the inhibitors Akti1/2 (43), rapamycin (43, 45), and Ku (46), to inhibit Akt, mTORC1 and mTORC1/2, respectively, blunted, as expected, the activation of S6K. However, despite strong inhibition of S6K, the CCR7-dependent phosphorylation of AMPK on Ser-485 was not affected (Fig. 5*D*). These results indicate that Akt, mTORC1, mTORC2, and S6K do not mediate CCR7-dependent inhibition of AMPK in mDCs (see model in Fig. 9).

CCR7-dependent Inhibition of AMPK in DCs Is Mediated by MEK/ERK—Upon stimulation of the mDCs with CCL21, we observed similar kinetics in the activation of the kinases MEK1/2/ERK1/2 and phosphorylation of AMPK on Ser-485 (Fig. 6*A*). Therefore, we studied whether MEK1/2/ERK1/2 could mediate the phosphorylation of AMPK on Ser-485 downstream of CCR7. Treatment of the cells with UO126 (Fig. 6*B*) or PD03255901 (Fig. 6*C*), two potent and selective inhibitors of MEK1/2 (45) and, consequently of ERK1/2, the only known downstream targets of MEK1/2 (47), blunted CCR7-dependent phosphorylation of AMPK, indicating that MEK1/2 regulates the phosphorylation of AMPK on Ser-485 downstream of CCR7. In the next experiments, we studied whether ERK1/2 could also regulate AMPK phosphorylation on Ser-485. Our attempts to reduce the expression of ERK1 or ERK2 in mDCs using siRNAs were unsuccessful. Although the siRNAs used readily blunted ERK1 and ERK2 expression in HL-60 cells, we were unable to reduce the levels of these two kinases in mDCs (not shown). Therefore, we decided to use two pharmacological inhibitors to block ERK1/2 activity, namely, CAY10561 (Fig. 7*A*) and FR180204 (Fig. 7*B*). CAY10561 displays a high selec-

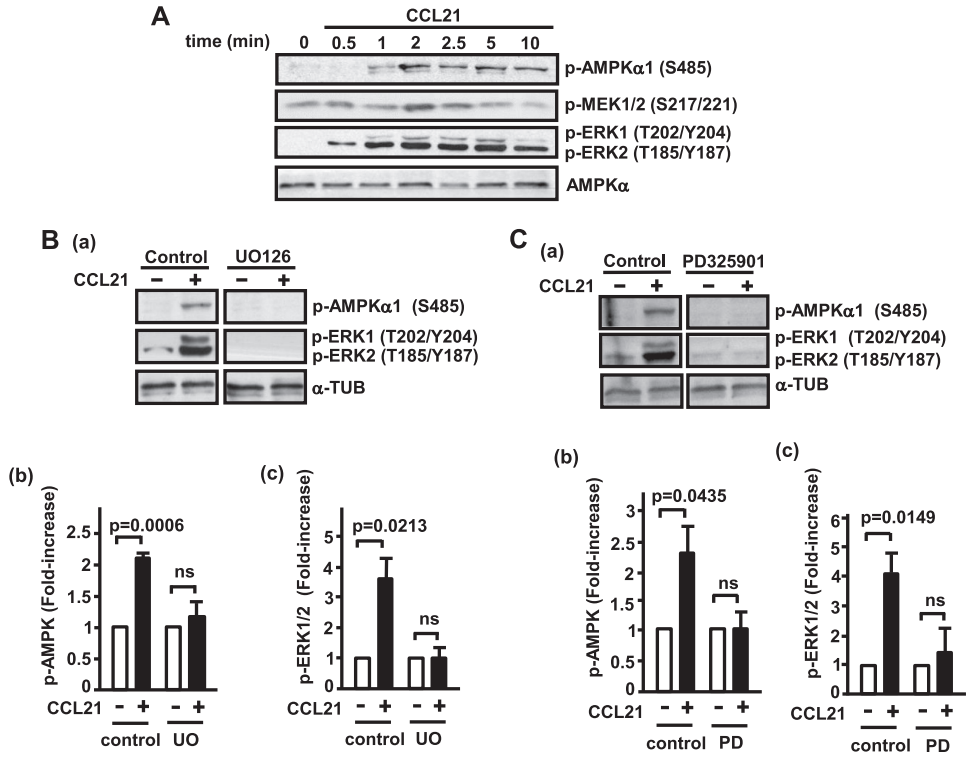

FIGURE 6. **CCR7-dependent phosphorylation/inhibition of AMPK is mediated by MEK.** *A*, DCs (100,000 cells) suspended in 0.1% BSA in RPMI were stimulated for the indicated times with CCL21 (15 nM) and then lysed and analyzed by SDS-PAGE, followed by Western blotting with Abs against phosphorylated AMPKα1 (Ser-485), MEK1/2 (Ser-217/221), or ERK1/2 (Thr-202/Thr-204 ERK1/Thr-185/Tyr-187 ERK2). To show equal loading, the membranes were reprobed with an Ab against AMPKα. A representative experiment out of three performed is shown. *B*, *panel a*, DCs suspended in 0.1% BSA in RPMI were either left untreated (*Control*) or pretreated with UO126 (2.5 μM, 60 min). The mDCs were subsequently stimulated or not with CCL21 for 5 min and then lysed, and the aliquots were subjected to Western blot with an antibody against phosphorylated/inactive AMPKα1 (Ser-485) or phosphorylated active ERK1/2 (Thr-202/Tyr-204 ERK1/Thr-185/Tyr-187 ERK2). α-Tubulin (α-*TUB*) levels show equal loading of the gels. A representative experiment out of three performed is shown. *Panel b*, -fold increase in the phosphorylation of AMPK in control and UO126 (*UO*)-treated mDCs, upon stimulation with CCL21. In both control and UO126-treated DCs, the degree of phosphorylation of the unstimulated DCs was given an arbitrary value of 1, and -fold increase in the CCL21-stimulated mDCs was represented. *Panel c*, similar to *panel b* with the difference that -fold increase in phosphorylation of ERK1/2 was examined. *C*, *panel a*, the experiments were performed as described in *B*, with the only difference that the DCs were treated with PD325901 (1 μM, 60 min). *Panels b* and *c*, similar to *panels b* and *c* in *B*, with the only difference that PD325901 was used. *ns* indicates non-significant differences.

tivity against ERK when tested against a panel of 184 related kinases (48, 49), and FR180 displays a high selectivity against ERK when tested against eight related kinases (50). As shown in Fig. 7, *A* and *B*, although the effects of CAY10561 and FR180 displayed higher variability when compared with the effects of the MEK1/2 inhibitors, both agents blocked CCR7-dependent phosphorylation of AMPK1a on Ser-485. Therefore, these results indicate that ERK1/2 can mediate the effects of MEK1/2 to induce inhibition of AMPK. As the pharmacological blocking of MEK1/2 and ERK1/2 prevents the phosphorylation/inhibition of AMPK, which plays pro-apoptotic roles, we predicted that treatment of the mDCs with the inhibitor would reduce the pro-survival effects induced by stimulation of CCR7. As shown in Fig. 7*C*, as expected, the pretreatment of the mDCs with the inhibitors of MEK1/2 or ERK1/2 reduced the pro-survival effects induced by the stimulation of CCR7, although at an extent slightly lower than that induced by inhibition of Akt.

ERK Associates to AMPK—As active MEK/ERK are required to observe phosphorylation of AMPK on Ser-485 downstream of CCR7, we studied the possibility that these molecules could associate to AMPKα in mDCs. We immunoprecipitated the endogenous AMPKα from cultures of mDCs and then carried out a Western blotting to analyze for the presence of ERK1 or MEK1 in the immunoprecipitates. As shown in Fig. 8*A*, we observed that AMPKα and ERK1 interacted both in unstimulated and in CCL21-stimulated mDCs, suggesting that these two proteins are able to associate, directly or indirectly, constitutively. In contrast, we did not detect MEK1 in the AMPKα immunoprecipitates (not shown). Because direct or indirect protein-protein associations cannot be discriminated by immunoprecipitation, to study whether AMPKα and ERK1 could interact directly each other, we performed a PLA (51, 52). This is a novel microscopy technique that allows detecting, with high specificity and sensitivity, close proximity between two proteins (<40 nm), suggesting direct interactions between these two molecules (30, 51, 52). The mDCs were plated on polyornithine-coated dishes, and then they were stimulated with CCL21 and finally subjected to a PLA analysis. Negative controls where single antibodies against ERK1 (Fig. 8*B*, *panel a*), AMPK1α (Fig. 8*B*, *panel a*), or MEK1 (Fig. 8*B*, *panel b*) were used showed no PLA fluorescence. Interestingly, we observed PLA fluorescence signal between the pair ERK1/AMPKα only in CCL21-stimulated mDCs, but not in unstimulated mDCs, suggesting that stimulation of CCR7 induces proximity between these two kinases (Fig. 8*B*, *panel c*). Consistent with immunoprecipitation results, we did not observe PLA fluorescent signal between the pair MEK1/AMPKα (not shown). Analysis of the interaction between ERK1 and MEK1, which was

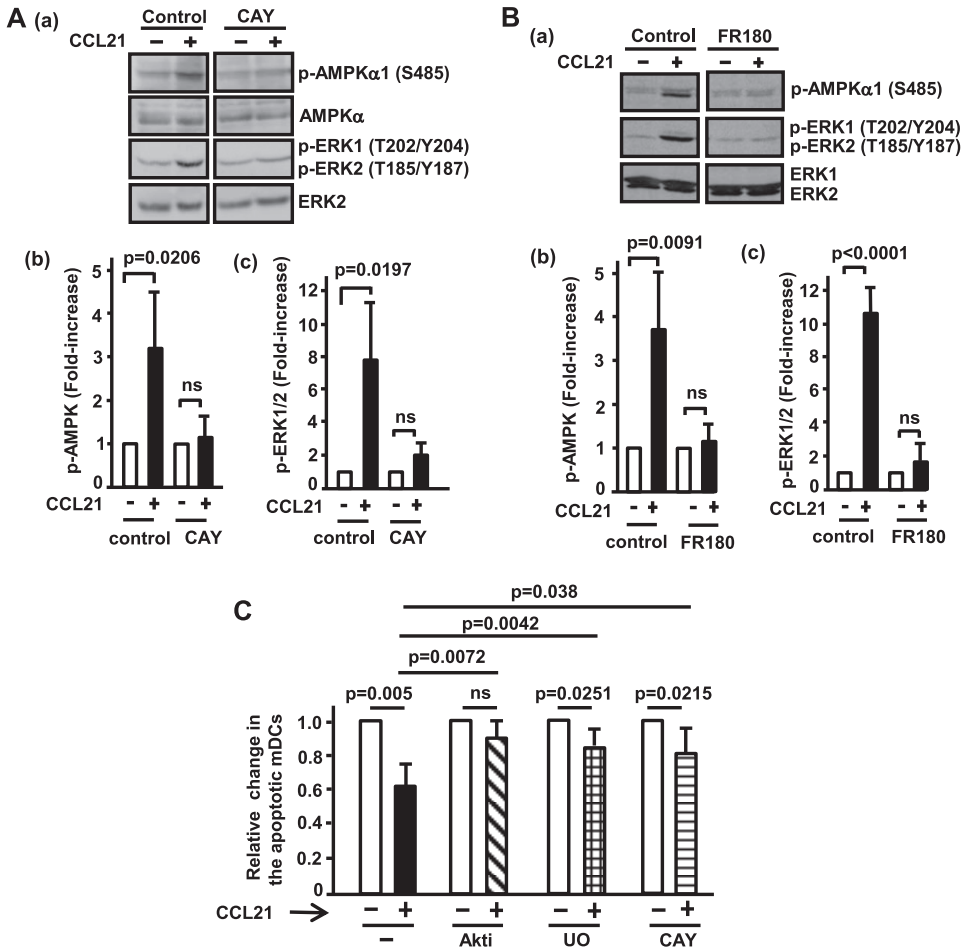

FIGURE 7. **CCR7-dependent phosphorylation/inhibition of AMPK is mediated by ERK.** *A*, *panel a*, DCs suspended in 0.1% BSA in RPMI were either left untreated (*Control*) or pretreated with CAY10561 (*CAY*, 20 μM, 2,5 h). The DCs were stimulated with CCL21 (15 nM) for 5 min and then lysed, and aliquots were subjected to Western blot with antibodies against phosphorylated/inactive AMPKα1 (Ser-485), total AMPKα, phosphorylated active ERK1/2 (Thr-202/Tyr-204 ERK1/Thr-185/Tyr-187 ERK2), or total ERK2. A representative experiment out of five performed is shown. *Panel b*, -fold increase in AMPK phosphorylation in control and CAY10561-treated mDCs, upon stimulation with CCL21. In both control and CAY10561-treated DCs, the degrees of phosphorylation of the unstimulated DCs were given an arbitrary value of 1, and the -fold increase in the CCL21-stimulated mDCs was represented. *Panel c*, similar to *panel b* with the difference that -fold increase in phosphorylation of Erk1/2 was examined. In *panels b* and *c*, the results represent the mean $\pm$ S.D. ($n = 5$ experiments). *ns* indicates non-significant differences. *B*, *panel a*, experiments were performed as described in *A*, with the differences that FR180 (100 μM, 60 min) was used and that anti-total ERK1/2 shows equal loading of the gels. A representative experiment out of three performed is shown. *Panel b*, similar to *panel b* in *A*, with the difference that -fold increase in AMPK phosphorylation was examined in the presence of FR180 as indicated in *panel a* in *B*. *Panel c*, experiments similar to *panel c* in *A* with the difference that -fold increase in phosphorylation of Erk1/2 was examined in the presence of FR180 as indicated in *panel a* in *B*. In *panels b* and *c*, the results represent the mean $\pm$ S.D. ($n = 3$ experiments). *ns* indicates non-significant differences. *C*, relative number of apoptotic DCs in unstimulated ($-$) and CCL21-stimulated DCs ($+$), after treating the mDCs with Akti, the MEK1/2 inhibitor UO126 (*UO*), or the ERK1/2 inhibitor CAY10561 (*CAY*). Results represent the mean $\pm$ S.D. ($n = 5$ experiments).

used as a positive control, also showed intense PLA fluorescence in the stimulated, but not in the unstimulated, mDCs (Fig. 8*B*, *panel d*). In summary, these results show that ERK and AMPK may be part of a similar protein complex, and in this complex, active ERK may control the phosphorylation of AMPK on Ser-485.

DISCUSSION

CCR7 directs mDCs to the LNs where the initiation of the immune response takes place. Previously, we showed that in addition to chemotaxis, CCR7 can promote survival in mDCs through the kinase Akt (10–12), which controls survival by inducing activation of NFκB and inhibition of FOXO1/3 and GSK3β (10–12). To get further insights on the mechanisms used by CCR7 to induce survival in mDCs, herein we have analyzed the involvement of the kinase AMPK in this process. Our results indicate that in mDCs, AMPK can play pro-apoptotic roles *in vitro* and *in vivo*.

The phenotypical features presented by the DCs that die after inducing activation of AMPK suggest that this kinase may induce an apoptotic type of death. In this regard, AMPK-dependent death is inhibited by the pan-caspase inhibitor z-VAD-FMK; it associates to caspase 3 activation, to the fragmentation of the nucleus, and to the increase in the expression of the pro-apoptotic Bcl2 family member Bim. Our results indicate that AMPK may promote apoptosis, at least partially, by inducing translocation to the nucleus of FOXO1, a transcription factor that plays pro-apoptotic roles in mDCs through the regulation of the expression of Bim (10, 25, 26), and by inhibiting mTORC1, a kinase complex controlled by CCR7 that also induces survival in mDCs (10, 26). In other cell types, AMPK has also been shown to be able to promote apoptosis using these two mechanisms (36, 53, 54).

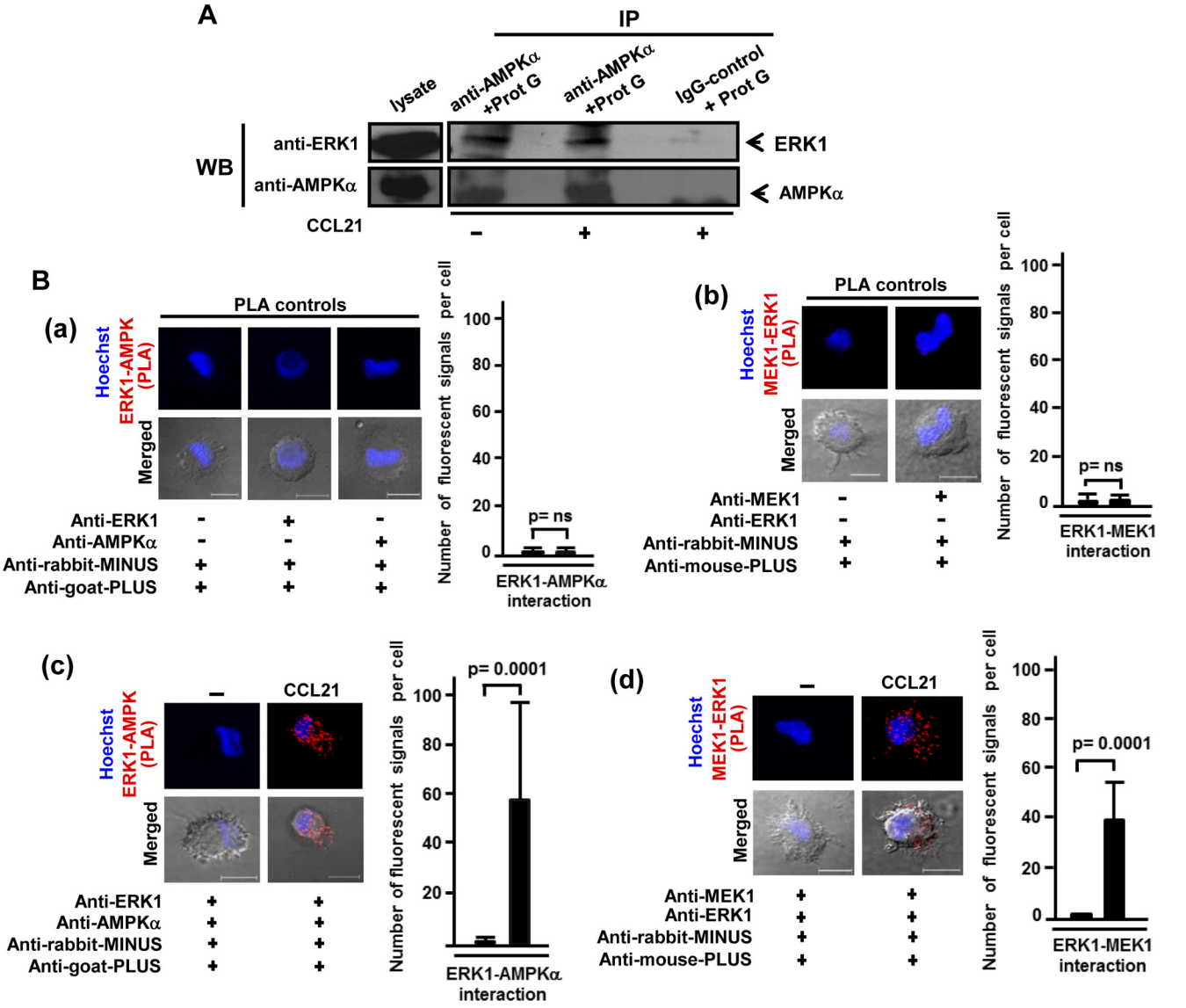

FIGURE 8. **AMPKα interacts with ERK1.** *A*, equal number of DCs, stimulated (+) or not (−) with CCL21 (15 nM), were subjected to immunoprecipitation (*IP*) with anti-AMPKα antibody or with IgG control, and subsequently, the immunoprecipitates were separated by SDS-PAGE, followed by Western blotting (*WB*) with anti-ERK1 or anti-AMPKα antibodies. A lysate of DCs was used as positive control. Aliquots of the lysates used to immunoprecipitate AMPK were analyzed for Western blotting for the presence of β-actin to demonstrate equal amount of proteins immunoprecipitated (not shown). *B*, interaction between ERK1 and AMPKα in mDCs was detected as fluorescent signals using the PLA. *Panels a* and *b*, PLA negative controls performed by labeling the DCs only with the anti-ERK1 or anti-AMPKα antibodies plus the anti-rabbit MINUS and the anti-goat PLUS (*panel a*) and the anti-MEK1 antibody and the anti-rabbit MINUS and the anti-mouse PLUS probes (*panel b*). Nomarski images and nuclei stained with Hoechst 33342 are also shown. *Scale bar*, 10 μm. In *panels a* and *b*, the number of fluorescent signals per cell was also quantified. At least 40 cells per field were counted. Results represent the mean ± S.D. ($n = 3$ experiments). *Panel c*, PLA fluorescent staining, indicating interaction between ERK1 and AMPKα, after CCL21 stimulation. *Panel d*, positive control. PLA fluorescent staining between MEK1 and ERK1 upon CCL21 stimulation is shown. Nomarski images and nuclei stained with Hoechst 33342 are also shown. *Scale bar*, 10 μm. In *panels c* and *d*, the number of fluorescent signals per cell was also quantified. At least 40 cells per field were counted. Results represent the mean ± S.D. ($n = 3$ experiments). *ns* indicates non-significant differences.

Consistent with its pro-survival role of the chemokine receptor CCR7 (11), we observed that its stimulation induces a rapid phosphorylation/inhibition of pro-apoptotic AMPK on Ser-485 (18–21). This inhibition of AMPK may promote DC survival through the effects that can be exerted on FOXO and mTORC1. Previously, we showed that stimulation of CCR7 induces activation of Akt, which, upon phosphorylating nuclear FOXO, induces its translocation to the cytoplasm (10, 11), preventing this factor from exerting pro-apoptotic effects through Bim. However, in contrast to Akt, active AMPK promotes, as shown above, the translocation of FOXO to the nucleus of DCs, from where it can regulate apoptosis. Thus, CCR7-mediated inhibition of AMPK may prevent this kinase from opposing the effects of Akt on FOXO, facilitating the complete translocation of FOXO to the cytoplasm. Moreover, CCR7-dependent inhibition of AMPK may also be able to prevent this kinase from inhibiting the pro-survival effects exerted by mTORC1. Thus, CCR7-mediated inhibition of AMPK may contribute to the extended survival of the DCs.

These results suggest that downstream of CCR7, the kinases MEK/ERK, but not Akt or S6K, mediate the phos-

phorylation of AMPK on Ser-485. Our results also indicate that ERK and AMPK may be components of a signaling complex where active ERK controls the phosphorylation of AMPK on Ser-485. Interestingly, these data contrast with prior results, obtained in other cell types, where it has been indicated that AMPK promotes inhibition of ERK (55–58), pointing out context-dependent differences in the mechanisms used by these two molecules to regulate each other. Previously, it has also been shown that infection of PK-15 cells with porcine circovirus type 2 (PCV2) also promotes interaction between AMPK and ERK (58). To the best of our knowledge, our work is the first study indicating that MEK/ERK can mediate the inhibition of AMPK by regulating Ser-485 phosphorylation.

The results obtained also indicate that MEK/ERK can regulate mDC survival. Until now, we had overlooked a role for MEK/ERK as regulators of CCR7-dependent survival in mDCs, probably due to the relatively less important role of these kinases as regulators of this function when compared with Akt. In most early experiments, the effects of MEK/ERK on mDC survival were analyzed after relatively short periods (6–10 h). Under these conditions, the effects of interfering with MEK/ERK on survival were negligible when compared with those induced by Akt inhibition. Only when apoptosis was analyzed after longer treatment with ERK1/2 inhibitors (24–40 h) did MEK/ERK emerge as a regulator of mDC survival, although still less potent than Akt. In Fig. 9, we present a model that summarizes the results obtained regarding the signaling mechanisms involved in the phosphorylation/inhibition of AMPK.

The results indicating that MEK/ERK, but not Akt, control AMPK phosphorylation on Ser-485 were unexpected for several reasons. First, we have shown previously that Akt is a key mediator of CCR7-dependent survival in mDCs (10, 11). Second, CCR7-mediated activation of Akt and phosphorylation of AMPK on Ser-485 were both mediated by G_i, suggesting that the CCR7-G_i-Akt axis may regulate the phosphorylation of AMPK. Third, Akt inhibits AMPK by directly phosphorylating Ser-485 on AMPK in several other cell types (18, 22, 23, 42). However, despite these prior results, we observe that inhibition of Akt or S6K, another kinase involved recently in the regulation of the phosphorylation of AMPK on Ser-485 (21), failed to block the phosphorylation of this residue upon stimulation of CCR7. In contrast, inhibition of MEK or its direct target ERK blocked CCR7-dependent phosphorylation of AMPK on Ser-485. Therefore, MEK/ERK emerge as novel regulators of the phosphorylation/inhibition of AMPK and, consequently, the survival of mDCs in addition to Akt. Interestingly MEK-ERK dependent phosphorylation of AMPK on Ser-485 seems cell- and/or receptor-specific because in granulosa cells, MEK/ERK inhibition was ineffective in preventing the FSH-mediated phosphorylation of AMPK on Ser-485 (22). These disparate results regarding the roles of Akt, S6K, and MEK/ERK on the phosphorylation of Ser-485 emphasize the combinatorial character of the signaling pathways and the importance of a detailed knowledge of the specific pathways used by specific receptors in each cell type. In summary, the data presented herein indicate that CCR7 may use the MEK-AMPK axis, in addition to Akt-dependent mechanisms (10–12), to promote survival in mDCs. These results add a novel component to the array of signals relayed from CCR7 to promote the survival of mDCs and provide new potential targets to modulate the function of these cells in the immune system.

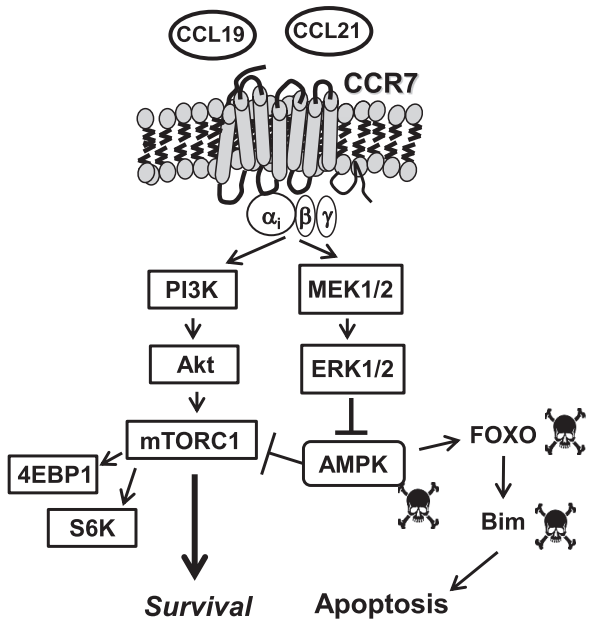

FIGURE 9. **CCR7-stimulated phosphorylation-inhibition of AMPK.** Stimulation of CCR7 with CCL19 or CCL21 induces $G_i G\beta\gamma$-mediated activation of the kinases MEK1/2/ERK1/2. CCR7 also induces activation of the PI3K/Akt/mTORC1/4EBP1 and S6K pathways, which promote survival in mDCs. Active AMPK induces apoptosis in mDCs by inhibiting the pro-survival effects of mTORC1 and by promoting translocation of the transcription factor FOXO to the nucleus, where it can control the expression of the pro-apoptotic Bcl2 family member Bim. Stimulation of CCR7 regulates, through the $G_i G\beta\gamma$/MEK1/2-ERK1/2 pathway (and independently of the PI3K/Akt/mTORC1pathway), the phosphorylation of the kinase AMPK on Ser-485, which results in the inhibition of this kinase and the consequent dampening of its pro-apoptotic effects. Therefore, CCR7 promotes survival in DCs through Akt-dependent mechanisms described previously (10–12) and by promoting MEK/ERK-dependent inhibition of AMPK.

Acknowledgments—We acknowledge P. Lastres for help with the cytometer and discussions and Génesis Andrea Altuve Urbina and Cristina Ruano Domínguez for expert technical assistance. We acknowledge Jill Suttles (University of Louisville School of Medicine) for kindly supplying reagents.

REFERENCES

1. Ueno, H., Klechevsky, E., Morita, R., Aspord, C., Cao, T., Matsui, T., Di Pucchio, T., Connolly, J., Fay, J. W., Pascual, V., Palucka, A. K., and Banchereau, J. (2007) Dendritic cell subsets in health and disease. *Immunol. Rev.* **219,** 118–142
2. Chen, M., Huang, L., and Wang, J. (2007) Deficiency of Bim in dendritic cells contributes to overactivation of lymphocytes and autoimmunity. *Blood* **109,** 4360–4367
3. Hildeman, D., Jorgensen, T., Kappler, J., and Marrack, P. (2007) Apoptosis and the homeostatic control of immune responses. *Curr. Opin. Immunol.* **19,** 516–521
4. Hou, W. S., and Van Parijs, L. (2004) A Bcl-2-dependent molecular timer regulates the lifespan and immunogenicity of dendritic cells. *Nat. Immunol.* **5,** 583–589
5. Nopora, A., and Brocker, T. (2002) Bcl-2 controls dendritic cell longevity *in vivo*. *J. Immunol.* **169,** 3006–3014

6. Ohnmacht, C., Pullner, A., King, S. B., Drexler, I., Meier, S., Brocker, T., and Voehringer, D. (2009) Constitutive ablation of dendritic cells breaks self-tolerance of CD4 T cells and results in spontaneous fatal autoimmunity. *J. Exp. Med.* **206,** 549–559
7. Kushwah, R., and Hu, J. (2010) Dendritic cell apoptosis: regulation of tolerance *versus* immunity. *J. Immunol.* **185,** 795–802
8. Randolph, G. J., Ochando, J., and Partida-Sánchez, S. (2008) Migration of dendritic cell subsets and their precursors. *Annu. Rev. Immunol.* **26,** 293–316
9. Comerford, I., Harata-Lee, Y., Bunting, M. D., Gregor, C., Kara, E. E., and McColl, S. R. (2013) A myriad of functions and complex regulation of the CCR7/CCL19/CCL21 chemokine axis in the adaptive immune system. *Cytokine Growth Factor Rev.* **24,** 269–283
10. Escribano, C., Delgado-Martín, C., and Rodríguez-Fernández, J. L. (2009) CCR7-dependent stimulation of survival in dendritic cells involves inhibition of GSK3β. *J. Immunol.* **183,** 6282–6295
11. Sánchez-Sánchez, N., Riol-Blanco, L., de la Rosa, G., Puig-Kröger, A., García-Bordas, J., Martín, D., Longo, N., Cuadrado, A., Cabañas, C., Corbí, A. L., Sánchez-Mateos, P., and Rodríguez-Fernández, J. L. (2004) Chemokine receptor CCR7 induces intracellular signaling that inhibits apoptosis of mature dendritic cells. *Blood* **104,** 619–625
12. Sánchez-Sánchez, N., Riol-Blanco, L., and Rodríguez-Fernández, J. L. (2006) The multiple personalities of the chemokine receptor CCR7 in dendritic cells. *J. Immunol.* **176,** 5153–5159
13. Hardie, D. G. (2011) AMP-activated protein kinase: an energy sensor that regulates all aspects of cell function. *Genes Dev.* **25,** 1895–1908
14. Hardie, D. G., Ross, F. A., and Hawley, S. A. (2012) AMPK: a nutrient and energy sensor that maintains energy homeostasis. *Nat. Rev. Mol. Cell Biol.* **13,** 251–262
15. Ido, Y., Carling, D., and Ruderman, N. (2002) Hyperglycemia-induced apoptosis in human umbilical vein endothelial cells: inhibition by the AMP-activated protein kinase activation. *Diabetes* **51,** 159–167
16. Campàs, C., Lopez, J. M., Santidrián, A. F., Barragán, M., Bellosillo, B., Colomer, D., and Gil, J. (2003) Acadesine activates AMPK and induces apoptosis in B-cell chronic lymphocytic leukemia cells but not in T lymphocytes. *Blood* **101,** 3674–3680
17. Woods, A., Vertommen, D., Neumann, D., Turk, R., Bayliss, J., Schlattner, U., Wallimann, T., Carling, D., and Rider, M. H. (2003) Identification of phosphorylation sites in AMP-activated protein kinase (AMPK) for upstream AMPK kinases and study of their roles by site-directed mutagenesis. *J. Biol. Chem.* **278,** 28434–28442
18. Horman, S., Vertommen, D., Heath, R., Neumann, D., Mouton, V., Woods, A., Schlattner, U., Wallimann, T., Carling, D., Hue, L., and Rider, M. H. (2006) Insulin antagonizes ischemia-induced Thr^{172} phosphorylation of AMP-activated protein kinase α-subunits in heart via hierarchical phosphorylation of $Ser^{485}/^{491}$. *J. Biol. Chem.* **281,** 5335–5340
19. Hurley, R. L., Barré, L. K., Wood, S. D., Anderson, K. A., Kemp, B. E., Means, A. R., and Witters, L. A. (2006) Regulation of AMP-activated protein kinase by multisite phosphorylation in response to agents that elevate cellular cAMP. *J. Biol. Chem.* **281,** 36662–36672
20. Pulinilkunnil, T., He, H., Kong, D., Asakura, K., Peroni, O. D., Lee, A., and Kahn, B. B. (2011) Adrenergic regulation of AMP-activated protein kinase in brown adipose tissue *in vivo*. *J. Biol. Chem.* **286,** 8798–9809
21. Dagon, Y., Hur, E., Zheng, B., Wellenstein, K., Cantley, L. C., and Kahn, B. B. (2012) p70S6 kinase phosphorylates AMPK on serine 491 to mediate leptin's effect on food intake. *Cell Metab.* **16,** 104–112
22. Kayampilly, P. P., and Menon, K. M. (2009) Follicle-stimulating hormone inhibits adenosine 5′-monophosphate-activated protein kinase activation and promotes cell proliferation of primary granulosa cells in culture through an Akt-dependent pathway. *Endocrinology* **150,** 929–935
23. Kovacic, S., Soltys, C. L., Barr, A. J., Shiojima, I., Walsh, K., and Dyck, J. R. (2003) Akt activity negatively regulates phosphorylation of AMP-activated protein kinase in the heart. *J. Biol. Chem.* **278,** 39422–39427
24. Zhou, G., Myers, R., Li, Y., Chen, Y., Shen, X., Fenyk-Melody, J., Wu, M., Ventre, J., Doebber, T., Fujii, N., Musi, N., Hirshman, M. F., Goodyear, L. J., and Moller, D. E. (2001) Role of AMP-activated protein kinase in mechanism of metformin action. *J. Clin. Invest.* **108,** 1167–1174
25. Delgado-Martín, C., Escribano, C., Pablos, J. L., Riol-Blanco, L., and Rodríguez-Fernández, J. L. (2011) Chemokine CXCL12 uses CXCR4 and a signaling core formed by bifunctional Akt, extracellular signal-regulated kinase (ERK)1/2, and mammalian target of rapamycin complex 1 (mTORC1) proteins to control chemotaxis and survival simultaneously in mature dendritic cells. *J. Biol. Chem.* **286,** 37222–37236
26. Riol-Blanco L, Delgado-Martín, C., Sánchez-Sánchez, N., Alonso-C, L. M., Gutiérrez-López, M. D., Del Hoyo, G. M., Navarro, J., Sánchez-Madrid, F., Cabañas, C., Sánchez-Mateos, P., and Rodríguez-Fernández, J. L. (2009) Immunological synapse formation inhibits, via NF-κB and FOXO1, the apoptosis of dendritic cells. *Nat. Immunol.* **10,** 753–760
27. Riol-Blanco, L., Sánchez-Sánchez, N., Torres, A., Tejedor, A., Narumiya, S., Corbí, A. L., Sánchez-Mateos, P., and Rodríguez-Fernández, J. L. (2005) The chemokine receptor CCR7 activates in dendritic cells two signaling modules that independently regulate chemotaxis and migratory speed. *J. Immunol.* **174,** 4070–4080
28. Nicoletti, I., Migliorati, G., Pagliacci, M. C., Grignani, F., and Riccardi, C. (1991) A rapid and simple method for measuring thymocyte apoptosis by propidium iodide staining and flow cytometry. *J. Immunol. Methods* **139,** 271–279
29. Riccardi, C., and Nicoletti, I. (2006) Analysis of apoptosis by propidium iodide staining and flow cytometry. *Nat. Protoc.* **1,** 1458–1461
30. Söderberg, O., Gullberg, M., Jarvius, M., Ridderstråle, K., Leuchowius, K. J., Jarvius, J., Wester, K., Hydbring, P., Bahram, F., Larsson, L. G., and Landegren, U. (2006) Direct observation of individual endogenous protein complexes *in situ* by proximity ligation. *Nat. Methods* **3,** 995–1000
31. Gómez-Cabañas, L., Delgado-Martín, C., López-Cotarelo, P., Escribano-Diaz, C., Alonso-C, L. M., Riol-Blanco, L., and Rodríguez-Fernández, J. L. (2014) Detecting apoptosis of leukocytes in mouse lymph nodes. *Nat. Protoc* **9,** 1102–1112
32. Mempel, T. R., Henrickson, S. E., and Von Andrian, U. H. (2004) T-cell priming by dendritic cells in lymph nodes occurs in three distinct phases. *Nature* **427,** 154–159
33. Corton, J. M., Gillespie, J. G., Hawley, S. A., and Hardie, D. G. (1995) 5-Aminoimidazole-4-carboxamide ribonucleoside: a specific method for activating AMP-activated protein kinase in intact cells? *Eur. J. Biochem.* **229,** 558–565
34. Winder, W. W., and Hardie, D. G. (1996) Inactivation of acetyl-CoA carboxylase and activation of AMP-activated protein kinase in muscle during exercise. *Am. J. Physiol.* **270,** E299–E304
35. Gilley, J., Coffer, P. J., and Ham, J. (2003) FOXO transcription factors directly activate *bim* gene expression and promote apoptosis in sympathetic neurons. *J. Cell Biol.* **162,** 613–622
36. Inoki, K., Zhu, T., and Guan, K. L. (2003) TSC2 mediates cellular energy response to control cell growth and survival. *Cell* **115,** 577–590
37. Gwinn, D. M., Shackelford, D. B., Egan, D. F., Mihaylova, M. M., Mery, A., Vasquez, D. S., Turk, B. E., and Shaw, R. J. (2008) AMPK phosphorylation of raptor mediates a metabolic checkpoint. *Mol. Cell* **30,** 214–226
38. Hung, C. M., Garcia-Haro, L., Sparks, C. A., and Guertin, D. A. (2012) mTOR-dependent cell survival mechanisms. *Cold Spring Harb. Perspect. Biol.* **4,** a008771
39. Kamath, A. T., Henri, S., Battye, F., Tough, D. F., and Shortman, K. (2002) Developmental kinetics and lifespan of dendritic cells in mouse lymphoid organs. *Blood* **100,** 1734–1741
40. Lehmann, D. M., Seneviratne, A. M., and Smrcka, A. V. (2008) Small molecule disruption of G protein $\beta\gamma$ subunit signaling inhibits neutrophil chemotaxis and inflammation. *Mol. Pharmacol.* **73,** 410–418
41. Iijima, N., Yanagawa, Y., Clingan, J. M., and Onoé, K. (2005) CCR7-mediated c-Jun N-terminal kinase activation regulates cell migration in mature dendritic cells. *Int. Immunol.* **17,** 1201–1212
42. Beauloye, C., Marsin, A. S., Bertrand, L., Krause, U., Hardie, D. G., Vanoverschelde, J. L., and Hue, L. (2001) Insulin antagonizes AMP-activated protein kinase activation by ischemia or anoxia in rat hearts, without affecting total adenine nucleotides. *FEBS Lett.* **505,** 348–352
43. Bain, J., Plater, L., Elliott, M., Shpiro, N., Hastie, C. J., McLauchlan, H., Klevernic, I., Arthur, J. S., Alessi, D. R., and Cohen, P. (2007) The selectivity of protein kinase inhibitors: a further update. *Biochem. J.* **408,** 297–315
44. Foster, K. G., and Fingar, D. C. (2010) Mammalian target of rapamycin (mTOR): conducing the cellular signaling symphony. *J. Biol. Chem.* **285,**

14071–14077
45. Davies, S. P., Reddy, H., Caivano, M., and Cohen, P. (2000) Specificity and mechanism of action of some commonly used protein kinase inhibitors. *Biochem. J.* **351,** 95–105
46. García-Martínez, J. M., Moran, J., Clarke, R. G., Gray, A., Cosulich, S. C., Chresta, C. M., and Alessi, D. R. (2009) Ku-0063794 is a specific inhibitor of the mammalian target of rapamycin (mTOR). *Biochem. J.* **421,** 29–42
47. Kolch, W. (2005) Coordinating ERK/MAPK signalling through scaffolds and inhibitors. *Nat. Rev. Mol. Cell Biol.* **6,** 827–837
48. Aronov, A. M., Baker, C., Bemis, G. W., Cao, J., Chen, G., Ford, P. J., Germann, U. A., Green, J., Hale, M. R., Jacobs, M., Janetka, J. W., Maltais, F., Martinez-Botella, G., Namchuk, M. N., Straub, J., Tang, Q., and Xie, X. (2007) Flipped out: structure-guided design of selective pyrazolylpyrrole ERK inhibitors. *J. Med. Chem.* **50,** 1280–1287
49. Hatzivassiliou, G., Liu, B., O'Brien, C., Spoerke, J. M., Hoeflich, K. P., Haverty, P. M., Soriano, R., Forrest, W. F., Heldens, S., Chen, H., Toy, K., Ha, C., Zhou, W., Song, K., Friedman, L. S., Amler, L. C., Hampton, G. M., Moffat, J., Belvin, M., and Lackner, M. R. (2012) ERK inhibition overcomes acquired resistance to MEK inhibitors. *Mol. Cancer Ther.* **11,** 1143–1154
50. Ohori, M., Kinoshita, T., Okubo, M., Sato, K., Yamazaki, A., Arakawa, H., Nishimura, S., Inamura, N., Nakajima, H., Neya, M., Miyake, H., and Fujii, T. (2005) Identification of a selective ERK inhibitor and structural determination of the inhibitor-ERK2 complex. *Biochem. Biophys. Res. Commun.* **336,** 357–363
51. Fredriksson, S., Gullberg, M., Jarvius, J., Olsson, C., Pietras, K., Gústafsdóttir, S. M., Ostman, A., and Landegren, U. (2002) Protein detection using proximity-dependent DNA ligation assays. *Nat. Biotechnol.* **20,** 473–477
52. Weibrecht, I., Leuchowius, K. J., Clausson, C. M., Conze, T., Jarvius, M., Howell, W. M., Kamali-Moghaddam, M., and Söderberg, O. (2010) Proximity ligation assays: a recent addition to the proteomics toolbox. *Expert Rev. Proteomics* **7,** 401–409
53. Greer, E. L., Oskoui, P. R., Banko, M. R., Maniar, J. M., Gygi, M. P., Gygi, S. P., and Brunet, A. (2007) The energy sensor AMP-activated protein kinase directly regulates the mammalian FOXO3 transcription factor. *J. Biol. Chem.* **282,** 30107–30119
54. Mihaylova, M. M., and Shaw, R. J. (2011) The AMPK signalling pathway coordinates cell growth, autophagy and metabolism. *Nat. Cell Biol.* **13,** 1016–1023
55. Du, J., Guan, T., Zhang, H., Xia, Y., Liu, F., and Zhang, Y. (2008) Inhibitory crosstalk between ERK and AMPK in the growth and proliferation of cardiac fibroblasts. *Biochem. Biophys. Res. Commun.* **368,** 402–407
56. Hwang, S. L., Jeong, Y. T., Li, X., Kim, Y. D., Lu, Y., Chang, Y. C., Lee, I. K., and Chang, H. W. (2013) Inhibitory cross-talk between the AMPK and ERK pathways mediates endoplasmic reticulum stress-induced insulin resistance in skeletal muscle. *Br. J. Pharmacol.* **169,** 69–81
57. Shen, C. H., Yuan, P., Perez-Lorenzo, R., Zhang, Y., Lee, S. X., Ou, Y., Asara, J. M., Cantley, L. C., and Zheng, B. (2013) Phosphorylation of BRAF by AMPK impairs BRAF-KSR1 association and cell proliferation. *Mol. Cell* **52,** 161–172
58. Zhu, B., Zhou, Y., Xu, F., Shuai, J., Li, X., and Fang, W. (2012) Porcine circovirus type 2 induces autophagy via the AMPK/ERK/TSC2/mTOR signaling pathway in PK-15 cells. *J. Virol.* **86,** 12003–12012